A Comprehensive Empirical Correlation for prediction of Supersolubility and Width of the Metastable Zone in Crystallization

Naser, Iraj *+

Science and Research Campus, Department of Chemical Engineering, Islamic Azad University, Hesarak, Poonak Tehran, I.R. IRAN

Manteghian, Mehrdad

Faculty of Engineering, Tarbiat Modarres University, P.O. Box 14155-4838, Tehran, I.R. IRAN

Bastani, Dariush

Department of Chemical Engineering, Sharif University of Technology, Tehran, I.R. IRAN

Mohammadzadeh, Mohsen

Faculty of Engineering, Tarbiat Modarres University, P.O. Box 14155-4838, Tehran, I.R. IRAN

ABSTRACT: *Prediction of supersolubility and the width of the metastable zone has been a major concern among the workers in the field of industrial crystallization. Operation of crystallizers under the optimum supersaturation low enough to attain the desired product quality (Median Particle Size, Crystal Size Distribution (CSD), Shape, Purity) being one motif. The inherent relationship between the subject and the most fundamental concepts of crystallization being the other. Studying the conditions of primary homogenous nucleation and the crystal growth kinetics has been conducted for a wide range of inorganic materials. A simple probabilistic term called chance of having the desirable species congregation, has been introduced to account for the effect of solution composition. A semi-empirical model has been developed for occasions where primary homogenous nucleation occurs at a specified undercooling rate (0.2 ^{o}C/hr). The model has been found to satisfy the experimental results obtained for 28 inorganic systems under various conditions. The concept may be equally applicable in nucleation of organic materials and for cases where liquid nuclei (such as rain droplets) are formed.*

KEY WORDS: *Particle formation, Nucleation, Supersolubility, Metastable zone, Modelling, Mathematical*

INTRODUCTION

The theoretical mechanism of primary homogenous nucleation has received the interest of many workers (Bradley[1], Nielsen [11], Walton [18,19], Dunning [4], Stauffer and Kiang [15], Burtun[2], Nishioka and Pound

* *To whom correspondence should be addressed.*
+ *E-mail: I.NASER@NAMVARAN.COM*
1021-9986/03/2/23 12/$/3.20

[12], Springer [14]). While the term "nucleation" has been used for both the birth of solids and liquids, the formation of liquid droplets from supersaturated vapour has received a comparatively wider level of consideration. A theoretical approach involves the assumption that molecules in the vapour phase combine to form embryos according to the reaction scheme:

$$A + A \leftrightarrow A_2$$
$$A_2 + A \leftrightarrow A_3$$
$$. \quad . \quad . \quad . \quad .$$
$$A_n + A \leftrightarrow A_{n+1}$$

The growth of the embryo continues accordingly in a supersaturated media until a certain size, called the critical size, is arrived at. Nuclei of this size are known to be in metastable equilibrium with their environment. A system of kinetic equations may then be solved to obtain the following expression for the nucleation rate (Burtun[2]).

$$J = \left(\sum_{N=1}^{\infty} \frac{1}{c_N b_N}\right)^{-1} \quad (1)$$

$$\sigma = -\frac{d(\ln c^*)}{d(\ln T)} \frac{\dot{T}}{T} t \quad (2)$$

Where b_N accounts for the probability of attachment of a vapour molecule to an embryo made up of N molecules in a single unit of time and c_N is the equilibrium concentration of an N-molecule embryo.

Study of the primary homogeneous nucleation of solids from solutions has so far been merely confined to speculations based on wild assumptions such as similarity of the behavior of gases and the dissolved molecules in a supersaturated solution. Mersmann and Bartosch [9] studied the secondary nucleation taking place in 28 inorganic systems. It was concluded that the visible shower of nuclei occurred at a volumetric hold-up of crystals between 10^{-4} and 10^{-3} and a corresponding size between 10 and 100 μm. An empirical model for prediction of the metastable zone width was then developed through a simple mathematical analysis. The model involved a roughly linear correlation between the relative supersaturation and time for cases when a constant cooling rate is applied (equation 2).

The correlation was then rearranged for cases where catalytic secondary nucleation and the integration-controlled growth were dominant. The model has been found to be more accurate in the case of steep solubility curves. Carlsson and Al Sacco [3] attempted to develop a model for the rates of nucleation and growth of zeolites from solutions by assuming one-, two-, or three-species responsible for nucleation and growth. The one-species mechanism assumes the presence of primary species (i.e., 2.5 nm amorphous particles) and crystalline zeolite only, where the primary species are responsible for both nucleation and growth. The two-species mechanisms assume, in addition to primary particles, the presence of amorphous colloidal aggregated species of 10 nm size in the crystallization system, and hypothesize their role in the nucleation and growth of zeolite crystals. The three-species mechanism assumes, in addition to the two-species mechanism, the possibility of growth from crystalline particles with size 10 nm.

Supersaturation curves for sodium nitrate and potassium nitrate were determined using a laser particle size analyzer by Graber and Taboada [7]. The curves were fairly parallel with the solubility curves and average ΔT values were 4.1 and 6.8 °C for potassium nitrate and sodium nitrate respectively. Ulrich and Strege [17] have reviewed the importance of determination of the width of the metastable zone and nucleation in industrial

THE THEORY

The theory is aimed to correlate the concentration at which a primary homogenous nucleation is observed with the following parameters:

1) *Probability of a favorable contact*, which is a new parameter. In order to explain this parameter, example is given for the nucleation in different aqueous solutions. In a brine solution, sodium and chloride ions co-exist with water molecules. Here the term "favorable contact" is meant by a situation where a chloride ion happens to be located beside a sodium ion be located. In the case of an aqueous solution of borax (sodium tetraborate decahydrate, $Na_2B_4O_7,10H_2O$) a favorable situation is achieved when two sodium ions happen to locate beside a tetraborate ion and ten water molecules. The probability of a "favorable contact" is the ratio of the chance of having such contacts on the total number of chances of contacts. In a stagnant 3-component solution having species A, B and C with their corresponding numbers N_A, N_B and N_C in the system the probability of favorable contact like $A_xB_yC_z$ can be computed through equation(3).

with $N = N_A + N_B + N_C$ being the total number of the species. The equation may be applied for inorganic salts in aqueous media where A and B represent the anion and the cation and C indicates water molecules. The product crystal may then be hydrated and contain z molecules of hydration water in its structure or be anhydrous for which $z = 0$.

For the case of crystallization of non-electrolyte A from solution B the first chance of nucleation is provided by a contact between two A species. The probability can be computed using equation (4).

In crystallization from pure melts the probability is always equal to unity.

2) *Agitation* is taken into consideration as the next effective parameter. In a non-stagnant solution, however, the effect of movement of the species should also be taken into account. In this work, the effect has been accounted for by incorporation of the agitator Reynolds number.

$$P = P(x, y, z) = \frac{(x + y + z)!}{x!\, y!\, z!}\left(\frac{N_A}{N}\right)^x \left(\frac{N_B}{N}\right)^y \left(\frac{N_C}{N}\right)^z \quad (3)$$

$$P = \left(\frac{N_A}{N}\right)^2 \quad (4)$$

$$C = A_0 + A_1 T^{B_0} + A_2 P^{B_1} + A_3 Re^{B_2} + A_4 G^{B_3} \quad (5)$$

3) *Temperature* is also given an account. When a favorable contact takes place, its stability should be allowed by the energetic state of the solution. Temperature is used to represent this energetic state of the solution.

4) Finally, the c*rystal growth rate* is considered as yet another effective parameter. In this study, the phenomenon of nucleation is detected by visual observation of a turbidity in the solution, and this is only possible when the embryo grows to a visible size.

The model is then suggested as equation (5) with T being the absolute temperature, P; the probability of suitable arrangement of the species, Re; the stirrer Reynolds number and G; the growth rate. Width of the metastable zone is then obtained by substraction of the solubility from the determined supersolubility.

THE EXPERIMENTS

A series of experiments were involved with derivation of solubility and supersolubility data for various systems. Further experiments were carried out to obtain growth rates for the same systems.

Determination of the Supersolubility

The supersolubility data were collected according to the method given by Nývlt [13]. The method involves preparation of a saturated solution through heating up solutions containing suspended crystals till they are dissolved and cooling them down again, until a turbidity is observed indicating the birth of new particles.

The apparatus is shown in Fig. 1. Both processes of dissolution and recrystallization were conducted in vessel A, a 15 l contoured-base cylindrical glass vessel stirred by an 8cm-blade propeller. The vessel diameter was 25 cm and its average height was 35 cm. It was immersed in a thermostatic water bath and was equipped with a stainless steel draft tube coaxially situated in it. The draft tube had an external diameter of 13cm and was supported in position by four vertical stainless steel baffles equally spaced in the annulus. It was a hollow tube and thermo-regulating water could be circulated inside it. The flow

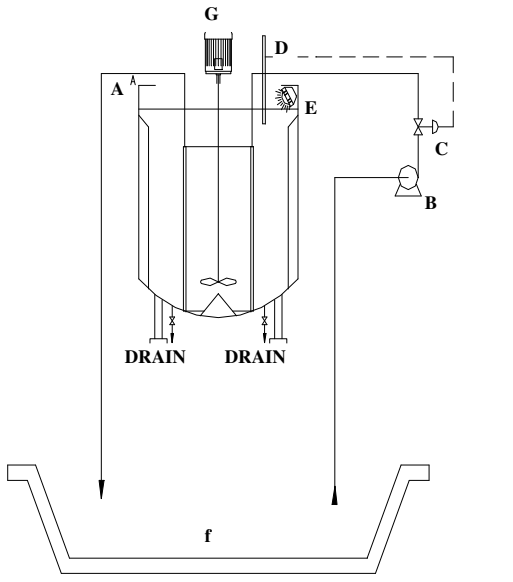

A DTB CRYSTALLISER
B PUMP
C CONTROL VALVE
D DIGITAL THERMOMETER
E LIGHT SOURCE
F VESSEL
G MOTOR

Fig.1: Set-up for measuring metastable limits in agitated vessels

rate of the water circulating inside the draft tube was controlled by the control valve C which received signals from the thermometer D installed in the vessel. Vertically beneath the draft tube was a cone with the same base diameter as the internal diameter of the draft tube. The cone served to divert the flow upward into the annulus. The vessel was initially fed with a roughly saturated solution. Initial cooling was then applied till fine crystals were observed in the vessel. The vessel was then heated so that the temperature rose at a set rate of 0.2 C^o/hr. The vessel content was observed carefully using a lamp lit above it. Disappearance of the last particles was considered as the saturation point. Cooling of the saturated solution was then conducted at a rate of 0.2 C^o/hr. The temperature at which crystal particles appeared in the solution was recorded (T´). The concentration of the solution initially fed into the vessel is now taken as the supersolubility corresponding to the recorded temperature (T´).

-By repetition of the above-mentioned procedures at the same stirrer speed but different temperatures, adequate solubility and supersolubility data were obtained and solubility-temperature (c vs. T) and supersolubility-temperature (c vs. T´) plots were drawn for the system corresponding to the particular stirrer speed.

-Repetition of the above procedures with changing the stirrer speeds resulted in a collection of the supersolubility data at a variety of agitation conditions. The stirrer speeds were chosen between 0-700 RPM with 100 RPM intervals.

Determination of the Growth Rate

Kinetics of growth of clusters and nuclei has been the subject of many studies. Mersmann and Bartosch [9] have shown that for an integration-controlled growth the displacement velocity of the crystal surface may be estimated through equation (6).

$$\upsilon = 2.25 \times 10^{-3} \nu^2 \frac{D_{AB}}{d_m} \frac{(c^*/c_c)^{4/3}}{\ln(c_c/c^*)} \sigma^2 \qquad (6)$$

An alternative method to measure the crystal growth rate is the method of initial derivatives. The method was mainly developed by Garside, Gibilaro and Tavare [6] and Tavare [16] and was further extended by Manteghian and Ebrahimi [8]. It is based on the temperature and solution concentration data obtained from a mixed batch cooling crystallizer seeded with monodispersed crystals. Initial derivatives of temperature and supersaturation are used in appropriate equations to yield the growth kinetics parameters. The growth rate in a batch crystallizer where the depletion in solute concentration is basically spent on growth is obtained from equation (7).

The crystal growth activation energy, E_g , the crystal growth order, g and the growth rate constant, K_g may be

Table 1: Growth kinetics correlations obtained for 28 inorganic systems

NO.	System	K_g*10^{-5}	E_g*10^{-3}	g	j	R^2
1	NH_4I	6250	-962	1.124	0.191	0.923
2	LiBr	6.62	-825	1.206	0.221	0.932
3	CsCl	2000	-938	1.324	0.235	0.935
4	$MgSO_4$	29.8	-786	1.211	0.207	0.954
5	KCl	1900	-912	1.224	0.245	0.925
6	$MgCl_2$	31.6	-698	1.311	0.211	0.984
7	$CuSO_4$	8.3	-758	1.281	0.201	0.975
8	NH_4Cl	2.22	-722	1.306	0.274	0.966
9	$NaBrO_3$	1.34	-722	1.266	0.218	0.922
10	NaBr	95.3	-725	1.276	0.281	0.934
11	$(NH_4)_2SO_4$	21.7	-710	1.255	0.277	0.978
12	$BaCl_2$	81.7	-692	1.222	0.311	0.954
13	$BeSO_4$	0.89	-751	1.212	0.233	0.965
14	$SrCl_2$	3.87	-736	1.226	0.261	0.966
15	$NaNO_2$	672	-870	1.346	0.288	0.945
16	$Ni(NO_3)_2$	675	-746	1.269	0.318	0.955
17	$KClO_3$	5.92	-716	1.224	0.338	0.977
18	$KBrO_3$	65.4	-750	1.206	0.291	0.959
19	LiCl	6.62	-705	1.119	0.270	0.966
20	$Pb(NO_3)_2$	78	-735	1.313	0.331	0.988
21	$CoSO_4$	7.72	-631	1.351	0.333	0.989
22	$NiSO_4$	610	-842	1.266	0.269	0.945
23	$NiBr_2$	630	-830	1.286	0.295	0.970
24	$Ba(NO_3)_2$	7.55	-693	1.231	0.222	0.945
25	$BaBr_2$	83	-841	1.111	0.224	0.942
26	K_2CO_3	6.13	-740	1.122	0.244	0.978
27	KI	7.52	-716	1.246	0.200	0.974
28	$NiCl_2$	650	-854	1.166	0.284	0.936

determined by evaluation of X_1, X_2 and X_3 defined as equations (8) to (11).

The values of K_g and X_1 to X_3 are determined by experimental evaluation of the initial temperature and supersaturation derivatives. In order to evaluate the growth order and the growth activation energy, these parameters are substituted in equation (12).

X_1/X_3 is then plotted v.s. X_2/X_3 and a straight line is fitted. The growth activation energy, E_g, is given by the intercept of this line. The slope of the line, on the other hand, gives the ratio $-gR_g / E_g$ from which the growth order g may be obtained. The growth rate kinetics equations are given in table 1. Assuming the same conditions (temperature, solution concentration, etc…), values of the growth rate were both calculated through equation (6) and through the models obtained based on the method of initial derivatives for the 28 inorganic salts listed in the first column in table 1. The values are plotted in fig. 2.

$$G = K_g \exp(-\frac{E_g}{R_g T})\Delta\omega^g N^j \quad (7)$$

$$X_1 = -\frac{(\Delta\dot{\omega}_0 + \sum_{i=0}^{n} i a_i \dot{T}_0 T_0^{i-1})\dot{T}_0 \alpha \overline{L}_0}{T_0^2} \quad (8)$$

$$X_2 = -\frac{(\Delta\dot{\omega}_0 + \sum_{i=0}^{n} i a_i \dot{T}_0 T_0^{i-1})\Delta\dot{\omega}_0 \alpha \overline{L}_0}{\Delta\omega_0} \quad (9)$$

$$X_3 = \{\Delta\ddot{\omega}_0 + \sum_{i=0}^{n} i a_i T_0^{i-2}[\ddot{T}_0 T_0 + (i-1)\dot{T}_0^2]\}\alpha \overline{L}_0 + \frac{(\Delta\dot{\omega}_0 + \sum_{i=0}^{n} i a_i \dot{T}_0 T_0^{i-1})^2}{A_{T_0}} \quad (10)$$

$$K_g = -\frac{\Delta\dot{\omega}_0 + \sum_{i=0}^{n} i a_i \dot{T}_0 T_0^{i-1}}{A_{T_0} \exp(-\frac{E_g}{R_g T_0})\Delta\Delta_0^g} \quad (11)$$

$$\frac{X_1}{X_3} = (-\frac{gR_g}{E_g})\frac{X_2}{X_3} - (\frac{R_g}{E_g}) \quad (12)$$

Supersolubility Values

Listed in the first column in table 1 are the systems tested. Fig. 3 represents the supersolubilities obtained for NH_4I aqueous solutions. The solid lines represent the results of a model derived when the data obtained for this system have been incorporated in a regressional analysis based on equation (5). Similar plots have been obtained for the rest of the systems and the results are given elsewhere (Naser [10]). Narrowing of the metastable zone width with increase of the stirrer speed is obvious in all figures. A selection of data has also been given in figures

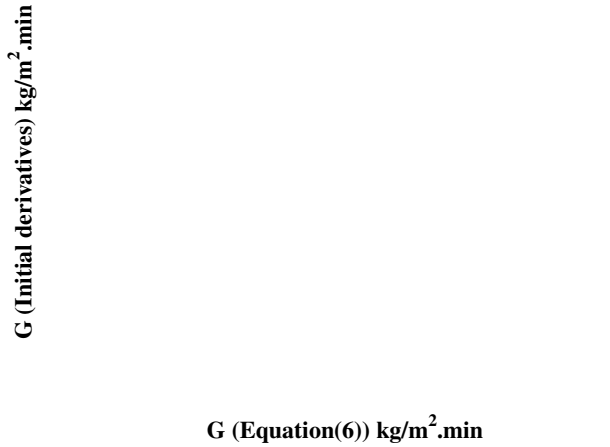

Fig. 2: Comparison of the growth rate obtained through the method of initial derivatives with the growth rate obtained through equation(6)

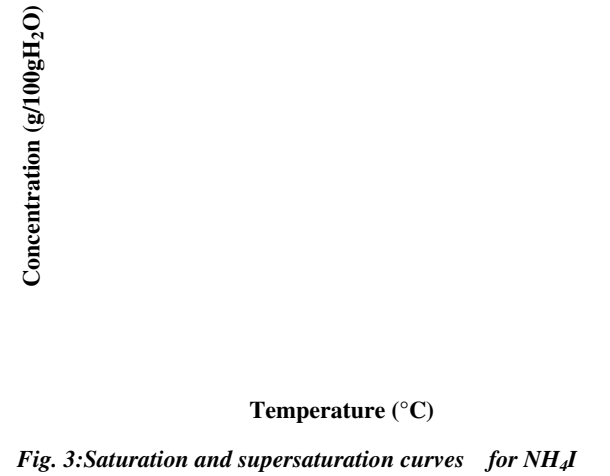

Fig. 3:Saturation and supersaturation curves for NH_4I

4 to 13. Results of a generalized model derived by incorporating the collection of data obtained in this work have also been shown in these figures. Details of the model derivation is given later in this paper.

Modeling

Modeling was initially achieved through direct application of the supersolubility values obtained through the experiments, the probability parameters calculated for each case, the temperatures and the growth rates measured in the foretold sections in a regressional analysis procedure. Next, dimensionless parameters were constructed with the effective variables and the regressional analysis was repeated with them.

Direct Regression

Fitting of equation (5) to the supersolubility data was accomplished using the software MATHEMATICA and the algorithm SOLVER developed by Larson and Waren (Fylstra, D., et al, [5]). A collection of data comprising the supersolubility, the stirrer speed, temperature, growth rate and the calculated probability of nucleation corresponding to the measured supersolubility were put in a unique data file. The program used the data to fit in equation (5). The criterion to optimize the parameters in a completely non-linear regression was to minimize the mean square of deviations defined as $(c_{exp}-c_{calc})$. The values of the coefficients and exponents in equation (5) obtained are as follows:

A_0=-451 A_1=8.1 A_2=255 A_3=4.9 A_4=155

B_0=0.594 B_1=0.2 B_2=-0.01 B_3=-0.01

and the model obtained is equation (13). As mentioned in the previous section the solid lines in figures 4 to 13 indicate predictions of the model for each system. Average deviations of the supersolubility values obtained through the model from those measured experimentally are given in table 2. According to the table, for 24 systems the average deviation of the model from the experimental results has remained below 14%. Nevertheles, for aqueous solutions of $MgCl_2$, $BeSO_4$, $NaNO_2$ and $NiCl_2$, the model has had an average deviation of 14% to 25% from the experimental results. This may be probably due to a more uniform solubility-temperature profile in the former systems. Analysis of the results shows that temperature, growth rate, the stirrer Reynolds number and the nucleation probability parameter have average response contributions of 40%, 15%, 15% and 30% respectively.

Dimensional Analysis

It was shown, both conceptually and experimentally, that a relationship exists between the supersolubility and certain physical and hydrodynamic properties. The next step is to explore similar correlations between dimensionless numbers that may be constructed with these parameters. Such dimensionless groups may be constructed using the following 8 parameters:

1	c	supersolubility	g solute/100g H_2O
2	P	nucleation probability	-
3	G	growth rate	$kg/m^2.min$
4	μ	solution viscosity	kg/m.s
5	D_{AB}	diffusivity	m^2/s
6	ρ	solution density	kg/m^3
7	N	agitation speed	s^{-1}
8	d	agitator diameter	m

Table 2: Average deviations of supersolubility values obtained through the model from the experimental values

NO.	System	Average Deviation(%)
1	NH_4I	13.00
2	LiBr	12.00
3	$BaBr_2$	13.00
4	CsCl	10.00
5	$MgSO_4$	9.00
6	KCl	11.00
7	$MgCl_2$	14.00
8	$CuSO_4$	12.00
9	NH_4Cl	6.00
10	$NaBrO_3$	8.00
11	NaBr	9.00
12	$(NH_4)_2SO_4$	8.00
13	$BaCl_2$	10.00
14	$Ba(NO_3)_2$	2.00
15	$BeSO_4$	15.00
16	$SrCl_2$	5.00
17	$NaNO_2$	17.00
18	$Ni(NO_3)_2$	11.00
19	KI	18.00
20	$KClO_3$	12.00
21	K_2CO_3	14.00
22	$KBrO_3$	12.00
23	$NiCl_2$	25.00
24	LiCl	9.00
25	$Pb(NO_3)_2$	8.00

26	$CoSO_4$	11.00
27	$NiSO_4$	11.00
28	$NiBr_2$	10.00

As there are 3 independent dimensions, the possible number of dimensionless numbers would be (8-3=5). P and C have been primarily nominated as two of them. A Buckingham $\prod$ theory analysis would then be needed to obtain the other 3.

Since mass transfer controls initial nucleation, solution density, the stirrer diameter and the molecular diffusivity have been used as repeating variables representing mass; system geometry and mass transfer effects. The dimensionless groups are therefore obtained by solving the equations (14) to (16).

The dimensionless groups obtained through solution of equations (14) to (16) are given after them. An effort to correlate these five dimensionless variables through a unified regressional analysis of the data obtained for all 28 systems was found to be unsuccessful. For the moderately soluble systems, comprising of: NaBr, $(NH_4)_2SO_4$, $BaCl_2$, $Ba(NO_3)_2$, $BeSO_4$, $SrCl_2$, $NaNO_2$, $KClO_3$, $KBrO_3$, LiCl, $CoSO_4$, $NiSO_4$, $MgSO_4$, KCl, $MgCl_2$, $CuSO_4$, NH_4Cl, $NaBrO_3$, $MgBr_2$, $BaBr_2$, K_2CO_3, $NiCl_2$, the following model (equation 17) was obtained with a correlation coefficient of 0.795. Comparisons between this model and equation (13) with the experimental results are shown in figures 14 to 19. The figures indicate that in general equation (13) is a better fit. The prediction of the dimensionless model, however, tends to approach the experimental results as the stirrer speed is increased. This may be an indication of the more profound effect of agitation. Analysis of the results shows that the nucleation probability, the stirrer Reynolds number, Peclet number and Sherwood number have average response contributions of 30%, 25%, 20% and 25% respectively.

$$C = 451 + 8.1T^{0.594} + 255P^{0.2} + 4.9Re^{-0.01} + 155G^{-0.01} \quad (13)$$

$$\prod_3 = d^a \rho^b D_{AB}{}^c G \quad (14)$$

$$\Pi_4 = d^a \rho^b D_{AB}{}^c N \quad (15)$$

$$\Pi_5 = d^a \rho^b D_{AB}{}^c \mu \quad (16)$$

$$\prod_3 = \frac{Gd}{\rho D_{AB}} = \text{Sherwood number (Sh)}$$

$$\Pi_4 = \frac{Nd^2}{D_{AB}} = \text{Peclet number (Pe)} = \text{Re.Sc}$$

$$\Pi_5 = \frac{\rho N d^2}{\mu} = \text{Reynolds number (Re)}$$

$$C = 2603 + 282Re^{0.0086} + 576P^{0.0144} - 197Pe^{0.01294} + 2042Sh^{0.0019} \quad (17)$$

Fig. 4: Comparison of the model with the experimental data for KCl, NH_4Cl and $CoSO_4$

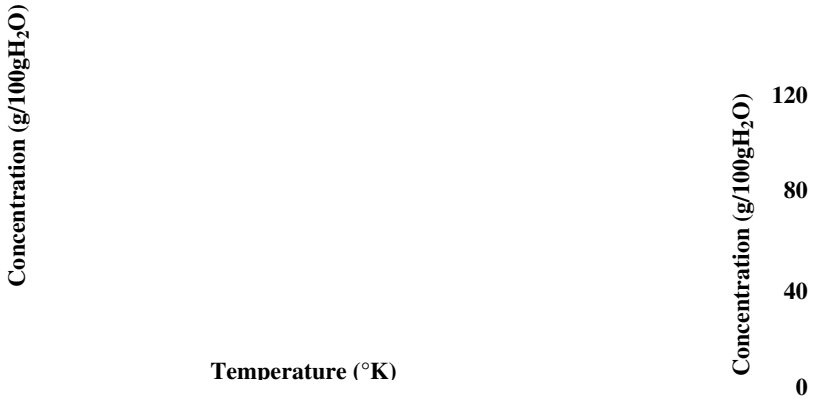

Fig. 5: Comparison of the model with the experimental data for $(NH_4)_2SO_4$, $KClO_3$ and $KBrO_3$

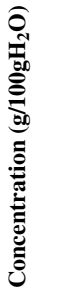

Fig. 6: Comparison of the model with the experimental data for $MgSO_4$, $MgCl_2$ and $NiSO_4$

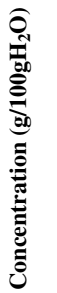

Fig. 7: Comparison of the model with the experimental data for $Ba(NO_3)_2$, $BeSO_4$ and $SrCl_2$

Fig. 8: Comparison of the model with the experimental data for $CuSO_4$, $NaBrO_3$ and $BaCl_2$

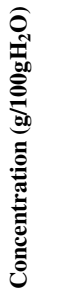

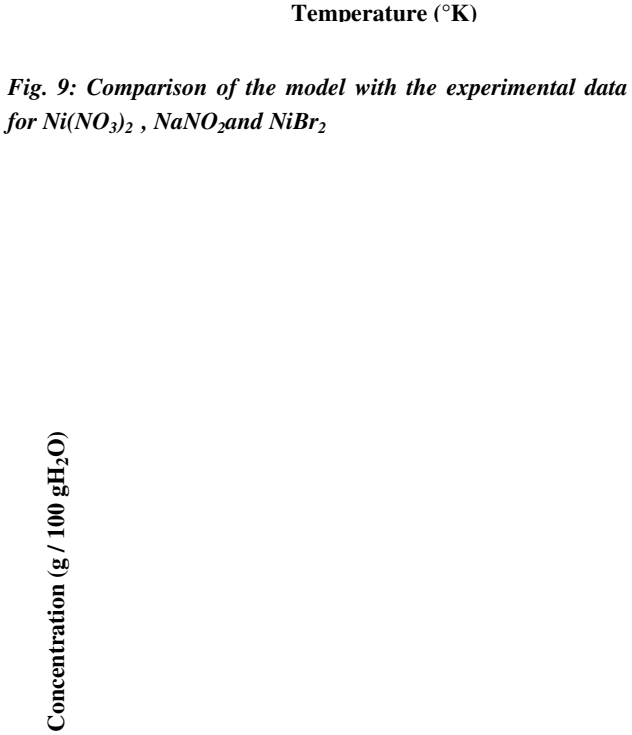

Fig. 9: Comparison of the model with the experimental data for $Ni(NO_3)_2$, $NaNO_2$and $NiBr_2$

Fig. 10: Comparison of the model with the experimental data for NaBr, LiCl and Pb $(NO_3)_2$

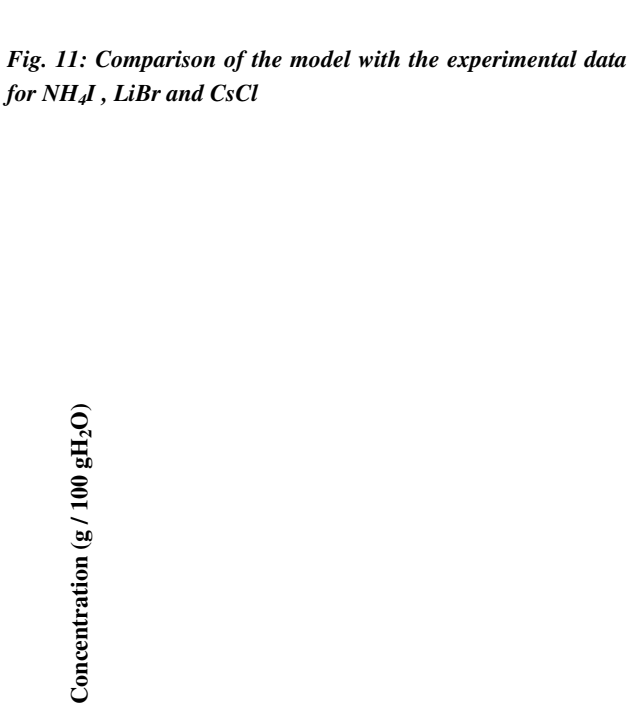

Fig. 11: Comparison of the model with the experimental data for NH_4I , LiBr and CsCl

Fig. 12: Comparison of the model with the experimental data for $BaBr_2$, K_2CO_3 and KI

Fig. 13: Comparison of the model with the experimental data for NiCl

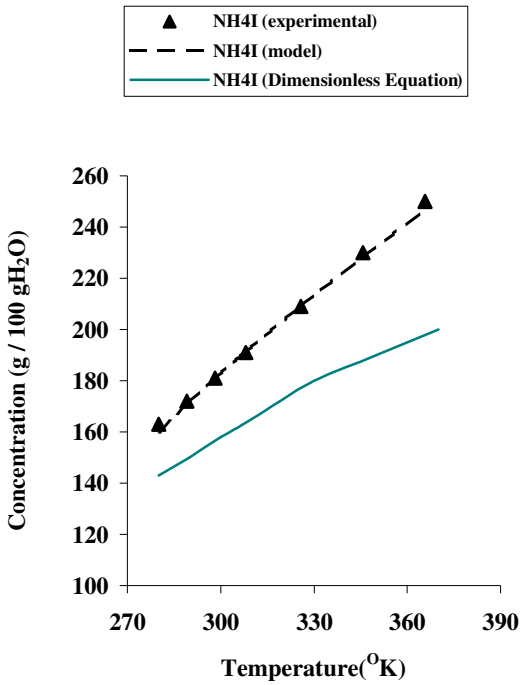

31

Fig. 14: Comparsion of the model (Eq. 13) and the dimensional analysis model with the experimental data for NH_4I at N=300 RPM

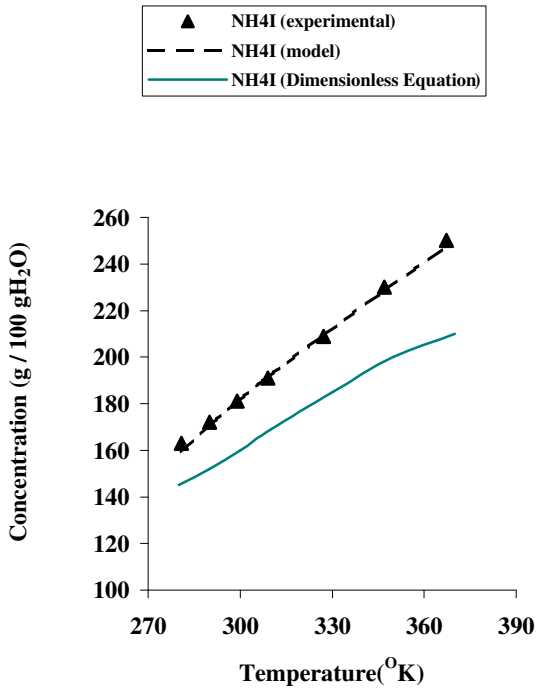

32

Fig. 15: Comparison of the model (Eq. 13) and the dimensional analysis model with the experimental data for NH4I at N=500 RPM

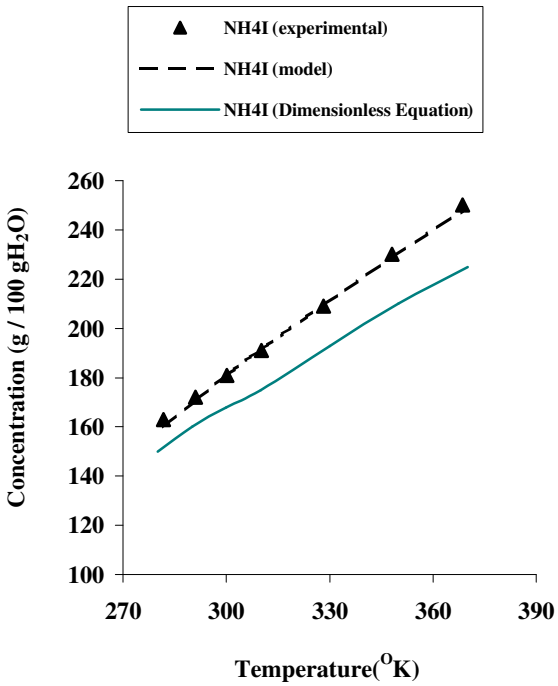

Fig. 16: Comparsion of the model (Eq. 13) and the dimensional analysis model with the experimental data for NH_4I at N=400 RPM

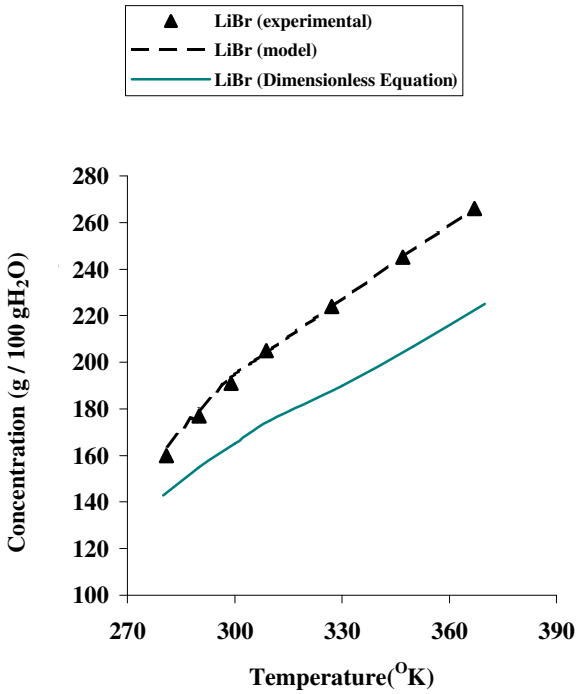

Fig. 17: Comparsion of the model (Eq. 13) and the dimensional analysis model with the experimental data for LiBr at N=300 RPM

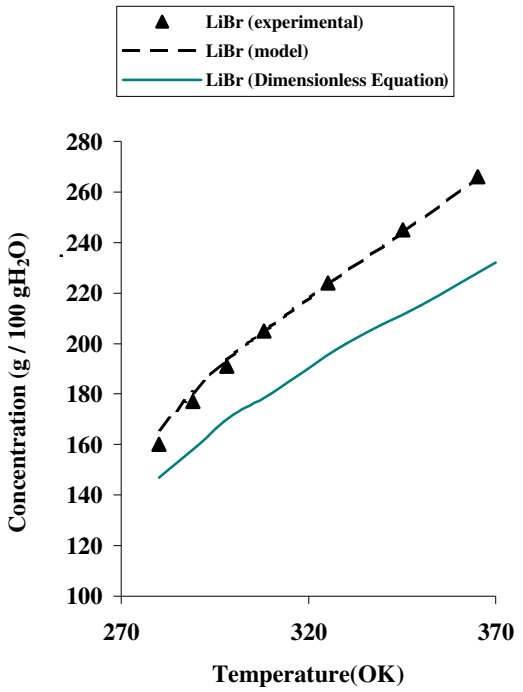

Fig. 18: Comparison of the model (Eq. 13) and the dimensionless model with the experimental data for LiBr at N=400 RPM

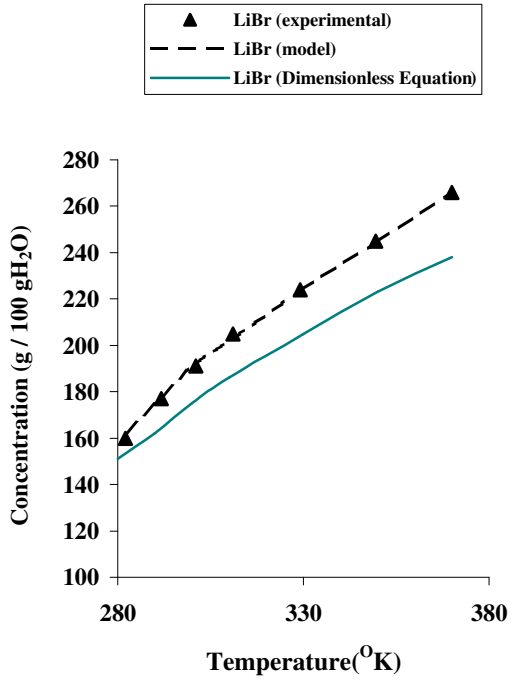

Fig. 19: Comparison of the model (Eq. 13) and the dimensionless model with the experimental data for LiBr at N=500 RPM

CONCLUSION

Through studying the figures 4 to 13 it may be concluded that the model expressed by equation (13) is a better fit in crystallization of aqueous solutions of $NiSO_4$, $CoSO_4$, NH_4Cl, KCl, $(NH_4)_2SO_4$, $NaBrO_3$, LiBr, $MgSO_4$, NaBr, $BaCl_2$, $Ba(NO_3)_2$, $BeSO_4$, $SrCl_2$, LiCl, $Pb(NO_3)_2$, NH_4I, CsCl, KI, K_2CO_3, $BaBr_2$, $KBrO_3$, $KClO_3$, $NaNO_2$ and $NiBr_2$ as compared to those of $MgCl_2$, $CuSO_4$, $Ni(NO_3)_2$, $NiCl_2$ and. This may be probably due to a more uniform solubility-temperature profile in the former systems. Compared to the generalized model (equation 13), the correlation derived among the dimensionless groups (equation 17) is less accurate.

The model shown by equation (13) can successfully predict the supersolubility diagram in most situations. The model, however does not seem to manage the systems having solubility-temperature diagrams with too variable slopes as successfully. A new parameter may be needed to compensate for such effects. The assumption of totally random congregation of the species may be further modified through accounting for the size and electric charge of the species.

List of symbols

A_T	total surface area of crystals
A	coefficient of the model polynomial
a	coefficient of first order term in the fitted polynomial T = f(t)
B	exponent of the model polynomial
b	coefficient of first order term in the fitted polynomial $\Delta c = g(t)$
b_N	probability of attachment of a vapor molecule to an embryo made up of N molecules in a single unit of time.
c_N	equilibrium concentration of an N-molecule embryo

c concentration, g/100gH_2O
d impeller diameter, m
d_m molecular diameter, m
D_{AB} Diffusivity, m^2/s
E_g crystal growth activation energy, kJ/mole
F crystal shape factor
G growth rate, kg/m^2.min
g crystal growth order
J nucleation rate, #/(s. unit solution weight)
K_g growth rate constant, kg/m^2.min
L crystal size, m
N number of species
P nucleation probability
R_g universal gas constant, 8.314kJ/mole.^oK
R^2 correlation coefficient, dimensionless
Re Reynolds number
Sc Schmidt number
Sh Sherwood number
T temperature, ^oK
t time, sec.
X_1,X_2, …parameters defined by equations 4 to
x,y,z stoichiometric coefficients of system under consideration

Greek letters

$\alpha = \frac{3\rho_s}{2F}$ crystal shape factor

Δ difference in a property
ρ_s crystal density, kg/m^3
ρ solution density, kg/m^3
μ viscosity, kg/m.s
ω concentration, gr/100grH_2O
ν number of ions per molecule, dimensionless
σ ≡ Δc/c*relative supersaturation, dimensionless
υ displacement velocity (2υ = G), m/s

Subscripts and superscripts

* saturation
c crystal
exp experimental
calc calculated
.&.. first and second derivatives
0 property at time 0
i, j subscripts and superscripts in fitted concentration, gr/100grH_2O

Received:29th December 2002 ; Accepted: 30th April 2003

REFERENCES

[1] Bradley, R. S. Quarterly rev., **5**, 315 (1951).
[2] Burtun, J.J., "Statistical Mechanics", ed. B.J. Berne, Plenum Press, New York p. 195 (1977).
[3] Carlsson, K. A. and Al Sacco Jr, J. W. *AIChE* 1999 New England Regional Conference (1999).
[4] Dunning, W.J., "In Nucleation", ed. A. C. Zettlemoyer, Marcel Dekker, New York p. 1 (1969).
[5] Fylstra, D .et al., *Interfaces*, **28**:5, 29 (1998).
[6] Garside, J., Gibilaro,L.G., Tavare, N.S., *Chem. Eng. Sci.,* **37**, 1625 (1982).
[7] Graber, T. A. and Taboada, M. E. *Cryst .Res. Technol*., **34**, 1269 (1999).
[8] Manteghian, M., Ebrahimi, A., "Solubility and Growth Kinetics of Silver Nitrate in Ethanol", International Conference on Mixing and Crystallization, Malaysia (1998).
[9] Mersmann, A. and Bartosch, K. *Journal of Crystal Growth*, **183** (1-2), 240 (1998).
[10] Naser, I. Ph.D. thesis, Islamic Azad University, Tehran (2002).
[11] Nielsen,A.E., "Kinetics of Precipitation",Pergamon, Oxford (1964).
[12] Nishioka, K. and Pound, G. M., *Advances in Colloid Interface Sci.,* **7**, 205 (1977).
[13] Nývlt, J.,"Industrial Crystallization from Solutions", London, Butterworths (1971).
[14] Springer, G. S.," Advances in Heat Transfer" ,**14**, 281 (1978).
[15] Stauffer, D. and Kiang, C. S., *Advances in Colloid Interface Sci*., **257**, 171 (1977).
[16] Tavare, N. S., *AICHE J.* , **31(10)**, 1733 (1985).
[17] Ulrich, J. and Stege, C., *Journal of Crystal Growth,* p. 237, 2130 (2002).
[18] Walton,A.G., "The Formation and Properties of Precipitates, Intersience", New York (1967).
[19] Walton, A. G., "In Nucleation", ed. A. C. Zettlemoyer, Marcel Dekker, New York p. 225, (1969).